Amplitude Calculation for 3-D Common Offset $v(z)$ Inversion

Meng Xu

19970717 096

DTIC QUALITY INSPECTED 3

DEPARTMENT OF THE NAVY
OFFICE OF NAVAL RESEARCH
SEATTLE REGIONAL OFFICE
1107 NE 45TH STREET, SUITE 350
SEATTLE WA 98105-4631

IN REPLY REFER TO:

4330
ONR 247
11 Jul 97

From: Director, Office of Naval Research, Seattle Regional Office, 1107 NE 45th St., Suite 350, Seattle, WA 98105

To: Defense Technical Center, Attn: P. Mawby, 8725 John J. Kingman Rd., Suite 0944, Ft. Belvoir, VA 22060-6218

Subj: RETURNED GRANTEE/CONTRACTOR TECHNICAL REPORTS

1. This confirms our conversations of 27 Feb 97 and 11 Jul 97. Enclosed are a number of technical reports which were returned to our agency for lack of clear distribution availability statement. This confirms that all reports are unclassified and are "APPROVED FOR PUBLIC RELEASE" with no restrictions.

2. Please contact me if you require additional information. My e-mail is *silverr@onr.navy.mil* and my phone is (206) 625-3196.

ROBERT J. SILVERMAN

Amplitude Calculation for 3-D Common Offset $v(z)$ Inversion

Meng Xu
Center for Wave Phenomena
Colorado School of Mines

ABSTRACT

The general 3-D inversion formula developed by Bleistein et al is specialized to a depth-dependent medium. An efficient ray tracer for this model is developed to calculate the necessary constituents of the ray theory. The traveltime and amplitude tables for the inversion are computed. The motivating application for this project is detection of small objects-10cm-in shallow water- 10-20m.

INTRODUCTION

This paper describes the background mathematical analysis for specialization of the Born/Kirchhoff inversion formalism [Cohen, Hagin and Bleistein, 1986; Bleistein, 1986], to a three dimensional (3-D) depth dependent background medium. Some numerical results that test the code I developed to implement this method are also presented.

The underlying motivating project has as its objective the detection of small objects (10-20cm) in shallow water (10-20m). This objective differs from the seismic inverse problem in two ways: first, the depth, time and frequencies differ from the seismic problem by approximately a factor of 100—not an important difference; second, the lateral extent of the scatterer is finite and small compared to the range from the source/receiver array or survey extent, whereas in the seismic problem, the lateral extent is often comparable to these other length scales. We have not, at this time, exploited this latter difference, so that the resulting code is applicable to both types of problems at both scales.

The survey we have in mind is traditional: a boat carries a towed array along parallel lines on the upper surface and periodically sets off an acoustic source, collecting the resulting backscattered data on the array. Data is then re-sorted in common (constant) offset data sets and processed by the program developed here to produce

a reflector map. In addition, the output provides an estimate of the angularly dependent reflection coefficient at specular at the sample points on the scatterer, as well as an estimate of that incident specular angle with respect to the normal to the reflector. By processing the data for a suite of offsets, data for amplitude versus offset (AVO) or amplitude versus angle (AVA) analysis is generated for each point on the reflector.

To calculate the amplitude weights for a 3-D common offset $v(z)$ inversion program, I use the analytic formulas for 3-D ray data in a depth dependent propagation medium. These ray data are interpolated from ray coordinates to cartesian coordinates after ray tracing. From these ray data, I compute the *Jacobian* of the transformation from Cartesian (x, y, z) coordinates to ray coordinates (σ, α, β) and I compute the Beylkin determinant h. Both of these determinants are essential to the amplitude computation.

The numerical tests confirm that the computer code matches analytical values of the travel time and amplitude along the rays extremely well. Furthermore, for a model sphere in constant background, we find that the reflector map successfully produces an image of the sphere.

INVERSION FORMULA

In this section, the inversion formulas of Bleistein [1986] are introduced. These formulas provide a tool for obtaining correct locatios of interfaces as well as a model-consistent specular reflection coefficient and incidence angle. The inversion formulas have the form of aperture-limited Fourier-like integrals. The integrand of these integrals contains a determinant that characterizes the viability of inverting a particular data set. This determinant is part of a Jacobian that depends on both the background propagation parameters and on the source-receiver configuration. As a result, the problem of extending the inversion formula to new recording geometries is reduced to a problem of computing the value of the form of this determinant that corresponds to a specific geometry.

The full 3-D Kirchhoff inversion formula Bleistein [1986] is

$$\beta(\mathbf{y}) = \frac{1}{8\pi^3} \int d^2\xi \frac{|h(\mathbf{y}, \xi)|}{a(\mathbf{y}, \xi)|\nabla_y \phi(\mathbf{y}, \xi)|} \int i\omega \, d\omega \, e^{-i\omega\phi(\mathbf{y}, \xi)} u_s(\mathbf{x}_g, \mathbf{x}_s, \omega). \tag{1}$$

In this equation, $\beta(\mathbf{y})$ is the reflectivity function for the imaging section; $\mathbf{y} = (y_1, y_2, y_3)$ is the 3-D position vector of the output or imaged point and $\xi = (\xi_1, \xi_2, 0)$ are the surface coordinates of the ray to $\mathbf{y}$ from either the source or receiver. For a common offset inversion, we denote by A_s and τ_s (A_g and τ_g) the amplitude and phase of the WKBJ Green's functions at $\mathbf{y}$ with initial point at the source. Thus, in the above equation

$$a(\mathbf{y}, \xi) = A_s A_g, \qquad \phi(\mathbf{y}, \xi) = \tau_s + \tau_g. \tag{2}$$

with the latter being the total traveltime from source to $\mathbf{y}$ to receiver. Furthermore, $u_s(\mathbf{x}_g, \mathbf{x}_s, \omega)$ is the data in ω (frequency) domain; $\mathbf{x}_s$ and $\mathbf{x}_g$ are the source and

the receiver position coordinates; h is the determinant characterize the viability of inverting a particular data set with a specific geometry at the given output point. The expression of the spatial weighting in terms of this one determinant for any source-receiver configuration and background propagation speed is a major contribution of Beylkin's approach to high-frequency inversion and is being referred as the "Beylkin determinant". The details of h will be described later.

The reflectivity function provides a reflectivity map through a family of bandlimited delta functions that peak on the reflectors in the medium. The peak amplitude is proportional to the angularly dependent reflection coefficient at a specular angle θ_s, where $2\theta_s$ is the angle between the ray directions from the source and receiver to the output point $\mathbf{y}$:

$$\beta_{peak} \sim R(\mathbf{y}, \theta_s) \frac{\cos\theta_s}{\pi c(\mathbf{y})} \int_{-\infty}^{\infty} F(\omega) d\omega. \tag{3}$$

That is, the peak value of β for $\mathbf{y}$ on S is the geometrical optics reflection coefficient multiplied by $2\cos\theta_s/c(\mathbf{y})$ and multiplied by $1/2\pi$ times the area under the filter in the ω-domain.

For $\mathbf{y}$ not on the reflector surface, the angle θ is defined by the equation,

$$\nabla_y \tau(\mathbf{y}, \mathbf{x}_s) \cdot \nabla_y \tau(\mathbf{y}, \mathbf{x}_g) = \frac{\cos 2\theta}{c^2(\mathbf{y})}. \tag{4}$$

Then, by computing $\nabla\phi(\mathbf{y}, \xi) \cdot \nabla\phi(\mathbf{y}, \xi)$, we are able to show that

$$|\nabla_y \phi(\mathbf{y}, \xi)| = \frac{2\cos\theta}{c(\mathbf{y})}. \tag{5}$$

In particular, for $\mathbf{y}$ on the reflector surface, this provides a means for estimating $\cos\theta_s$, through the introduction of another inversion operator, differing from β by one power of $|\nabla_y \phi|$:

$$\beta_1(\mathbf{y}) = \frac{1}{8\pi^3} \int d^2\xi \frac{|h(\mathbf{y}, \xi)|}{a(\mathbf{y}, \xi)|\nabla_y \phi(\mathbf{y}, \xi)|^2} \int i\omega \, d\omega \, e^{-i\omega\phi(\mathbf{y}, \xi)} u_S(\mathbf{x}_g, \mathbf{x}_s, \omega). \tag{6}$$

The addition of the extra divisor of $|\nabla_y \phi|$ introduces this divisor in the asymptotic amplitudes of the result. In particular:

$$\beta_{1peak}(\mathbf{y}) \sim R(\mathbf{y}, \theta_s) \frac{1}{2\pi} \int F(\omega) \, d\omega, \tag{7}$$

The fact that these two operators differ by a factor of $2\cos\theta/c(\mathbf{y})$ allows us to estimate $\cos\theta_s$ from the ratio of the outputs without ever having determined the specular source-receiver pair that produced the distinguished value of θ_s. This, in turn allows us to determine $R(\mathbf{y}, \theta_s)$ from either output. With knowledge of θ_s and the background wavespeed, $c(\mathbf{y})$, it is conceivable, within the limits of the accuracy of the data, that we should be able to estimate the jump in the propagation speed across the reflector using the formula for the geometrical optics reflection coefficient. More generally, in a variable density medium, we determine the impedance jump from this analysis. By processing data for multiple offsets, we generate data for amplitude versus offset (AVO) analysis or amplitude versus angle (AVA) analysis.
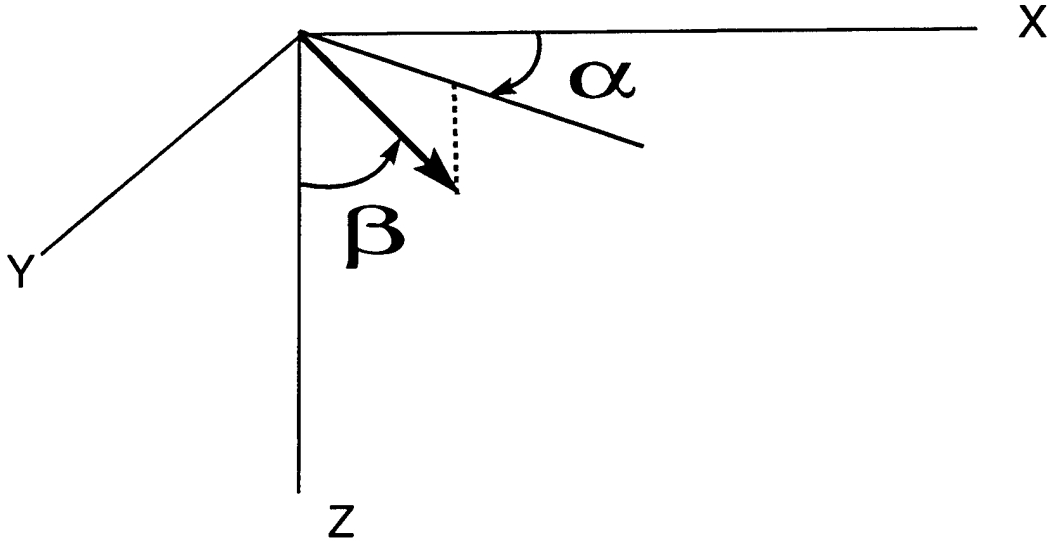
FIG. 1. Diagram of coordinate system showing an initial ray direction.

RAY TRACING

Here, I describe the ray tracing in a depth-dependent medium in 3-D. For a more complete discussion of the underlying ray theory for determining solutions of the wave equation in the form $A \exp[i\omega\tau]$, refer to Bleistein [1984].

The ray equations

The general form of the ray equations

$$\frac{dx_i}{d\sigma} = p_i, \qquad \frac{dp_i}{d\sigma} = p\frac{dp}{dx_i}, \quad i = 1, 2, 3,$$

$$\frac{d\tau}{d\sigma} = p^2, \quad p_1{}^2 + p_2{}^2 + p_3{}^2 = \frac{1}{c^2} \equiv p^2. \tag{8}$$

provide the basis for ray theoretic modeling.

The *slowness* vector $\mathbf{p} \equiv \bigtriangledown \tau$ points in the direction normal to the surfaces of constant τ. Surfaces of constant τ are called "wavefronts", and the $\mathbf{p}$ vector points in the direction tangent to the "raypaths". These, in turn, are the spatial trajectories of the solution to (8).

We seek solutions of (8) for rays emanating from a single point, say x_0, y_0, z_0 in an arbitrary downward direction. Those directions are determined by the initial values of α and β representing the azimuthal and polar angles, respectively, of the spherical coordinate system. See Fig. 1. Then, the initial ray direction $\mathbf{p_0}$ is given by

$$\mathbf{p_0} \equiv p_0(\cos\alpha\sin\beta, \sin\alpha\sin\beta, \cos\beta). \tag{9}$$

Specialization to a Depth-dependent medium

For a medium that has wavespeed variability only in the z direction, p_1 and p_2 are constants on each ray path; denote them by p_{10} and p_{20}. Note that p_{10} and p_{20} are their respective initial values.The ray equations become

$$\frac{dx_1}{d\sigma} = p_{10}, \qquad \frac{dx_2}{d\sigma} = p_{20}, \qquad \frac{dx_3}{d\sigma} = p_3,$$

$$\frac{dp_1}{d\sigma} = 0, \qquad \frac{dp_2}{d\sigma} = 0, \qquad \frac{dp_3}{d\sigma} = p\frac{dp}{dx_3}, \tag{10}$$

$$\frac{d\tau}{d\sigma} = p^2.$$

From the eikonal equation, we know the value of p_3

$$
\begin{aligned}
p_3 &= \sqrt{p^2(x_3) - p_{10}^2 - p_{20}^2} \\
&= \sqrt{p^2(x_3) - p^2(x_{30})\sin^2\beta}.
\end{aligned}
\tag{11}
$$

The third equation in (10) relates σ and x_3, so the ray equations may be rewritten in terms of x_3:

$$\frac{dx_1}{dx_3} = \frac{p_{10}}{p_3}, \qquad \frac{dx_2}{dx_3} = \frac{p_{20}}{p_3},$$

$$\frac{dp_1}{dx_3} = 0, \qquad \frac{dp_2}{dx_3} = 0, \tag{12}$$

$$\frac{dp_3}{dx_3} = \frac{p}{p_3}\frac{dp}{dx_3},$$

$$\frac{d\tau}{dx_3} = \frac{p^2}{p_3}, \qquad \frac{d\sigma}{dx_3} = \frac{1}{p_3}.$$

We solve for x_1, x_2, τ, and σ as functions of x_3, α, and β. Let the initial depth be $x_{30} \equiv z_0$ and the final depth be $x_3 \equiv z$. The solution of (13), then, is

$$x - x_0 = \frac{\cos\alpha\sin\beta}{c(z_0)} \int_{z_0}^{z} \frac{dz'}{\sqrt{p^2(z') - p^2(z_0)\sin^2\beta}},$$

$$y - y_0 = \frac{\sin\alpha\sin\beta}{c(z_0)} \int_{z_0}^{z} \frac{dz'}{\sqrt{p^2(z') - p^2(z_0)\sin^2\beta}},$$

$$\tag{13}$$

$$\tau - \tau_0 = \int_{z_0}^{z} \frac{dz'}{c^2(z')\sqrt{p^2(z') - p^2(z_0)\sin^2\beta}},$$

$$\sigma - \sigma_0 = \int_{z_0}^{z} \frac{dz'}{\sqrt{p^2(z') - p^2(z_0)\sin^2\beta}}.$$

Recall that α and β are the initial angles of the ray. When $p_3 = 0$, the ray is horizontally propagating. This is called a "turning point". The equations above all have integrable singularities at the turning point, requiring special care in numerical computation, to be discussed below.

The Jacobian J and Ray Amplitude

Here, I discuss the solution of the transport equation

$$2\nabla\tau \cdot \nabla A + A\nabla^2\tau = 0, \tag{14}$$

for the amplitude A. This equation can also be written as an ordinary differential equation in the ray parameter σ

$$\frac{d(A^2 J)}{d\sigma} = 0, \tag{15}$$

with solution (Bleistein 1984, 8.3.12)

$$A = \frac{\sqrt{\sin\beta}}{4\pi\sqrt{c(\xi)J(\sigma,\alpha,\beta)}}. \tag{16}$$

In these equations, J is the Jacobian of the transformation from $\mathbf{x}$ to (σ,α,β) via the solution of the ray equations,

$$J = \left| \frac{\partial(x,y,z)}{\partial(\sigma,\alpha,\beta)} \right|. \tag{17}$$

We calculate the ray theoretic amplitude A by computing J.

Let us consider the solution of the ray equations in terms of σ, rather than z. The solution is a family of rays, distinguished from one another by the choice of the parameters α and β. Along each ray, the values of τ, σ, x, y, z, p_i are known. p_1 and p_2 are constants on each ray; that is, independent of σ:

$$p_1 = \frac{1}{c(z_0)}\cos\alpha\sin\beta,$$

$$\tag{18}$$

$$p_2 = \frac{1}{c(z_0)}\sin\alpha\sin\beta.$$

With p_1 and p_2 independent of σ, the equations for x and y are

$$x = \xi_1 + \frac{\sigma}{c(z_0)} \cos\alpha \sin\beta,$$

$$y = \xi_2 + \frac{\sigma}{c(z_0)} \sin\alpha \sin\beta. \tag{19}$$

and z is given in terms of σ by

$$z = \int p_3 d\sigma. \tag{20}$$

I do not use equation (20) since we do the calculation on a uniform z grid, instead, we calculate σ for each z by using the third equation in (10). From (20) and (10), we can derive the nine terms of the determinant J in (17) as

$$\frac{\partial x}{\partial\sigma} = \frac{\sin\beta \cos\alpha}{c(z_0)},$$

$$\frac{\partial y}{\partial\sigma} = \frac{\sin\beta \sin\alpha}{c(z_0)},$$

$$\frac{\partial z}{\partial\sigma} = p_3,$$

$$\frac{\partial x}{\partial\alpha} = -\frac{\sigma\sin\beta \sin\alpha}{c(z_0)},$$

$$\frac{\partial y}{\partial\alpha} = \frac{\sigma\sin\beta \cos\alpha}{c(z_0)},$$

$$\frac{\partial z}{\partial\alpha} = 0, \tag{21}$$

$$\frac{\partial x}{\partial\beta} = \frac{\sigma\cos\beta \cos\alpha}{c(z_0)},$$

$$\frac{\partial y}{\partial\beta} = \frac{\sigma\cos\beta \sin\alpha}{c(z_0)},$$

$$\frac{\partial z}{\partial\beta} = \int \frac{-\sin\beta}{c(z_0)} d\sigma.$$

With these values, we can calculate J in (16) and then calculate A by using (17). Thus, we obtain A on a uniform grid in z, but calculate it as if the independent parameter along the ray were σ.

The Belkyin determinant h

The effects of source-receiver geometry are completely described by the Beylkin determinant

$$h(y,\xi) = \det \begin{bmatrix} \mathbf{p}_s + \mathbf{p}_g \\ \dfrac{\partial(\mathbf{p}_s + \mathbf{p}_g)}{\partial \xi_1} \\ \dfrac{\partial(\mathbf{p}_s + \mathbf{p}_g)}{\partial \xi_2} \end{bmatrix}, \tag{22}$$

in terms of the slowness vectors $\mathbf{p}_s$ and $\mathbf{p}_g$ and their derivatives with respect to the surface coordinates, (ξ_1, ξ_2). These vector quantities are evaluated at the output point $\mathbf{y}$.

The determinant must be finite and nonzero for the identification of the cascaded model and inversion integral as an approximate Fourier transform. Thus, we could use the value of this matrix to characterize source-receiver configurations as providing invertible data by this formalism at an output point, $\mathbf{y}$. In particular, we require that this determinant be finite and nonzero for some range of ξ values at any $\mathbf{y}$ where the high frequency inversion is to be computed.

The general form of the Beylkin determinant can be written for all source receiver geometries as

$$\begin{aligned} h(y,\xi) &= (p_s + p_g) \cdot (v_s + v_g) \times (w_s + w_g) \\ &= (p_s + p_g) \cdot v_g \times w_g + \\ &\quad (p_s + p_g) \cdot v_s \times w_s + \\ &\quad (p_s + p_g) \cdot v_g \times w_s + \\ &\quad (p_s + p_g) \cdot v_s \times w_g. \end{aligned} \tag{23}$$

where,

$$v_s \equiv \frac{\partial p_s}{\partial \xi_1}, \quad v_g \equiv \frac{\partial p_g}{\partial \xi_1},$$

$$\tag{24}$$

$$w_s \equiv \frac{\partial p_s}{\partial \xi_2}, \quad w_g \equiv \frac{\partial p_g}{\partial \xi_2}.$$

The first two terms can be recognized as being the Beylkin determinants for the common shot and common receiver geometries. We may write the Beylkin determinant as

$$\begin{aligned} h(y,\xi) = 2\cos^2\theta \left[h_s(y,\xi) + h_g(y,\xi) \right] + \\ (p_s + p_g) \cdot \left[v_g \times w_s + v_s \times w_g \right], \end{aligned} \tag{25}$$

where $h_g(y,\xi) = p_g \cdot v_g \times w_g$ is the determinant for the common receiver case and $h_s(y,\xi) = p_s \cdot v_s \times w_s$ is the determinant for the common source case. Unfortunately, the last term in (26) contains the cross products $v_s \times w_g$ and $v_g \times w_s$, which are not easily simplified.

Another way of writing the Beylkin determinant is

$$
\begin{aligned}
h(y,\xi) \;=\;& 2\cos^2\theta\,[h_s(y,\xi)+h_g(y,\xi)] \\
& +h_a(y,\xi)+h_b(y,\xi) \\
& +h_c(y,\xi)+h_d(y,\xi),
\end{aligned} \tag{26}
$$

where the h_a, h_b, h_c and h_d are defined by

$$
h_a(y,\xi) \equiv p_s \cdot v_s \times w_g, \quad h_b(y,\xi) \equiv p_s \cdot v_g \times w_s,
$$

$$
h_c(y,\xi) \equiv p_g \cdot v_g \times w_s, \quad h_d(y,\xi) \equiv p_g \cdot v_s \times w_g. \tag{27}
$$

Unfortunately, we cannot write the general common-offset Beylkin determinant in a form that has a common multiplier of $\cos^2\theta$.

We already know the vectors $\mathbf{p}_s$ and $\mathbf{p}_g$ at the output point from the solution of the ray equations. Now we will compute their partial derivatives with respect to ξ_1 and ξ_2 as solutions of another set of ray equations.

By taking derivatives of (19) with respect to ξ_1 and ξ_2, respectively, and using (20), we obtain differential equations for $\partial p_1/\partial \xi_i$ and $\partial p_2/\partial \xi_i$. These equations are

$$
\begin{aligned}
\frac{\partial p_1}{\partial \xi_1} &= -(1+p_1\frac{\partial \sigma}{\partial \xi_1})/\sigma, \\
\frac{\partial p_2}{\partial \xi_1} &= -p_2\frac{\partial \sigma}{\partial \xi_1}/\sigma, \\
\frac{\partial p_1}{\partial \xi_2} &= -p_1\frac{\partial \sigma}{\partial \xi_2}/\sigma, \\
\frac{\partial p_2}{\partial \xi_2} &= -(1+p_2\frac{\partial \sigma}{\partial \xi_2})/\sigma.
\end{aligned} \tag{28}
$$

The only quantities that we do not know in the above equations are $\partial\sigma/\partial\xi_1$ and $\partial\sigma/\partial\xi_2$. It is difficult to implement the derivatives with respect to ξ_1 and ξ_2. However, using the symmetry of the $v(z)$ medium, we find that $d/d\xi_1 = -d/dx$ and $d/d\xi_2 = -d/dy$ as shown schematically in Fig. 2. That is, when a ray is shifted horizontally, the quantity σ on that ray does not change. Also, one can see from Fig. 2, $d\sigma/d\xi = (\sigma_1 - \sigma_2)/d\xi = -(\sigma_2 - \sigma_1)/dx$. Thus, $\partial\sigma/\partial/\xi_1$ and $\partial\sigma/\partial/\xi_2$ are determined from results already calculated.

From the eikonal equation–the last equation in (8), the derivatives of p_3 with respect to ξ_1 and ξ_2 can also be found:

$$
\frac{\partial p_3}{\partial \xi_1} = -(p_1\frac{\partial p_1}{\partial \xi_1} + p_2\frac{\partial p_2}{\partial \xi_1})/p_3,
$$
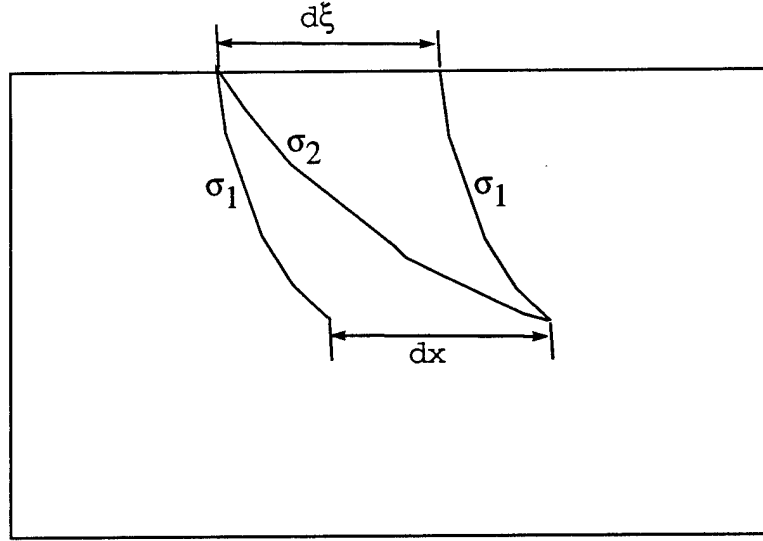
FIG. 2. Ray symmetry used in calculating h

$$\frac{\partial p_3}{\partial \xi_2} = -(p_1 \frac{\partial p_1}{\partial \xi_2} + p_2 \frac{\partial p_2}{\partial \xi_2})/p_3.$$

<div align="right">(29)</div>

The derivatives for source and receiver are calculated seperately using (28) and (29). There is a certain symmetry here that can be exploited since the difference between the source and the receiver is just a shift in x. Once we have h, together with the product of ray theoretic amplitudes, a in 1 and 2, the amplitude computation is complete.

NUMERICAL IMPLEMENTATION

Ray data are generated along each raypath with a unique coordinate reference (α, β, σ). Transformation of ray data from this ray system to a uniform grid is achieved by linear interpolation as shown in Fig. 3. Rays intersect with a z-plane. Four adjacent intersection points that surround a grid point are found. Linear interpolation is used to determine the ray data at the grid point from the four intersection points.

This scheme is not accurate in the vicinity where rays are near turning because the distance between the intersection points will be too large. To deal with rays propagating nearly horizontally, that is, when p_3 is small, vertical interpolation is used. Vertical interpolation differs from the above scheme in that it use a vertical plane instead of a horizontal z-plane. The nearly horizontally propagating rays will intersect the vertical plane with a closer spacing leading to a more accurate interpolation than if we used a horizontal interpolation grid.

Now we have all the ray data we need on the uniform (x, y, z) grid. Use these ray data to calculate the Jacobian J, ray amplitude a and Beylkin determinant h.
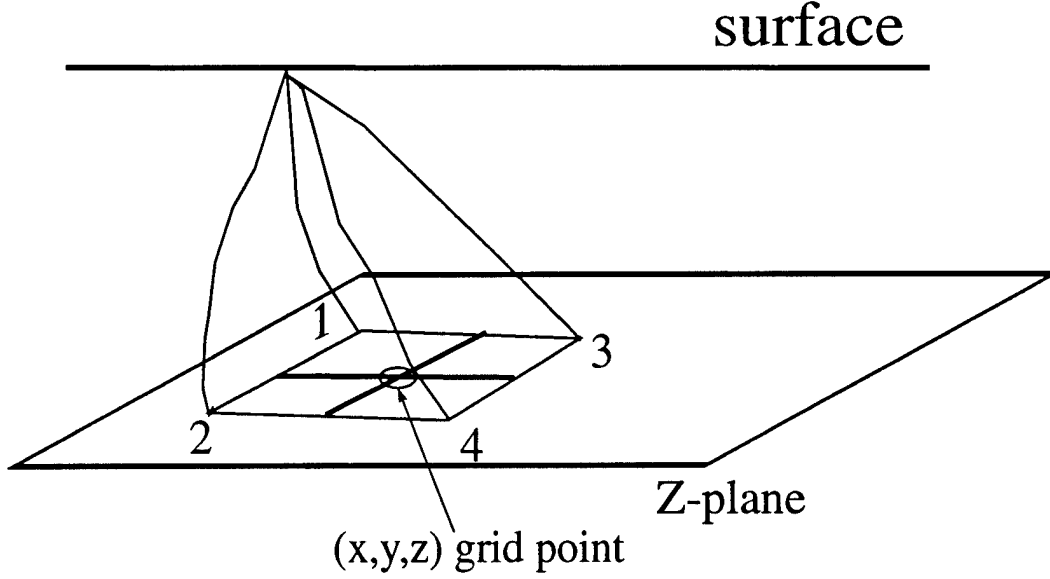
surface

FIG. 3. Diagram of interpolation from ray coordinate to uniform grid points.

Combining these values gives the amplitude weight value at each grid point for that particular source point. This amplitude table along with the traveltime table will be used in the inversion, it is just a shift and interpolation for other source or receiver points as the ray data are invariant for lateral displacement.

EXAMPLE: CONSTANT WAVESPEED

In this section, we present the specialization of the above results for a constant wavespeed medium where all calculations can be carried out explicitly. in this case, equation (17) reduces to

$$J = \frac{r^2}{c} \sin \beta, \tag{30}$$

and equation (16) becomes,

$$A = \frac{1}{4\pi r}. \tag{31}$$

For the special case of constant-wavespeed, with a generally non-flat surface, some simplification of h is possible. Application of Gaussian elimination produces the following simplified forms for h_a, h_b, h_c, and h_d in (27)

$$
\begin{aligned}
h_a(y, \xi) &\equiv \frac{-1}{c^3 r_s} \hat{r}_s \cdot \frac{\partial x_s}{\partial \xi_1} \times \frac{\partial p_g}{\partial \xi_2}, \\
h_b(y, \xi) &\equiv \frac{-1}{c^3 r_s} \hat{r}_s \cdot \frac{\partial p_g}{\partial \xi_1} \times \frac{\partial x_s}{\partial \xi_2}, \\
h_c(y, \xi) &\equiv \frac{-1}{c^3 r_g} \hat{r}_g \cdot \frac{\partial p_s}{\partial \xi_1} \times \frac{\partial x_g}{\partial \xi_2},
\end{aligned}
\tag{32}
$$

11

$$h_d(y,\xi) \equiv \frac{-1}{c^3 r_g} \hat{r}_g \cdot \frac{\partial x_g}{\partial \xi_1} \times \frac{\partial p_s}{\partial \xi_2}.$$

For the special case of constant wavespeed, with a flat recording surface, h_s, h_g, h_a, h_b, h_c, and h_d become

$$h_g \equiv \frac{y_3}{c^3 r_g^3}, \qquad h_s \equiv \frac{y_3}{c^3 r_s^3},$$

$$h_a \equiv \frac{y_3}{c^3 r_s^2 r_g}, \qquad h_b \equiv \frac{y_3 \cos 2\theta}{c^3 r_s r_g^2}, \tag{33}$$

$$h_c \equiv \frac{y_3 \cos 2\theta}{c^3 r_s^2 r_g}, \qquad h_d \equiv \frac{y_3}{c^3 r_s r_g^2}.$$

Substituting these results into equation (26), the full expression for the Beylkin determinant may be written as

$$h(y,\xi) = 2\cos^2\theta \, \frac{y_3}{c^3} \left[\frac{(r_s + r_g)(r_s^2 + r_g^2)}{r_s^3 r_g^3} \right] \tag{34}$$

The corresponding formulas for $\beta(y)$ and $\beta_1(y)$ for 3D common-offset, constant-wavespeed, and with a flat recording surface become

$$\beta(y) = \frac{2y_3}{c^2 \pi} \int d^2\xi \left[\frac{(r_s + r_g)(r_s^2 + r_g^2)}{r_s^2 r_g^2} \right] \cos\theta$$

$$\int i\omega \, d\omega \, e^{-i\omega[r_s + r_g]/c} u_S(x_g, x_s, \omega), \tag{35}$$

and

$$\beta_1(y) = \frac{y_3}{c\pi} \int d^2\xi \left[\frac{(r_s + r_g)(r_s^2 + r_g^2)}{r_s^2 r_g^2} \right]$$

$$\int i\omega \, d\omega \, e^{-i\omega[r_s + r_g]/c} u_S(x_g, x_s, \omega). \tag{36}$$

Equation (36) exactly matches equation (30) in Sullivan and Cohen [1987], which was derived using a different approach.

Below is a list of comparison of the numerical results and the analytic results of a constant background. The grids are $40 \times 40 \times 40$ and the ray shooting grids in α and β are 15×15, which is rather coarse. The numerical results have two or three digit accuracy:

Depth	Analytic	Numerical	Error
$4\Delta z$	0.059402	0.062488	5.19%
$8\Delta z$	0.287655	0.291268	1.26%
$12\Delta z$	0.483947	0.490268	1.31%
$16\Delta z$	0.638489	0.644558	0.95%
$20\Delta z$	0.754078	0.759777	0.76%
$24\Delta z$	0.838724	0.843727	0.60%
$28\Delta z$	0.900615	0.905202	0.51%
$32\Delta z$	0.946287	0.950361	0.43%
$36\Delta z$	0.980478	0.983688	0.33%
$40\Delta z$	1.017178	1.020043	0.28%

These are the amplitude weights on one trace (with a 4-sample skip) at offset $10\Delta z$. Notice that the accuracy increases with depth, this is because the polar angle β associated with the rays increases with depth and thus has a closer ray spacing for interpolation. The computation of travel time was about 10 times more accurate.

INVERSION EXAMPLES

The first example provides a simple test of positioning and amplitude accuracy. The model consists of constant velocity layers, as shown in Figure 4. Layer velocities are 2, 3, 6 and 10km/s from the top to the bottom. Figure 5 shows the model data with offset=3km. The inversion produces two outputs: one for β and one for β_1. The amplitudes in the two outputs differ by the factor $\cos\theta$, where θ is the specular angle. For the first interface, the real values: R is 0.200, $R\cos\theta$ is 0.172 and θ is 30.90 degrees. The inversion results: R is 0.203, $R\cos\theta$ is 0.174 and θ is 30.84 degrees. The percentage errors are 1.5, 1.1 and 0.2 percent respectively. For the second interface, the exact values: R is 0.333, $R\cos\theta$ is 0.307 and θ is 22.76 degrees. The inversion results: R is 0.341, $R\cos\theta$ is 0.315 and θ is 22.71 degrees. The percentage errors are 2.4, 2.6 and 0.2 percent respectively. For the third interface, the exact values: R is 0.250, $R\cos\theta$ is 0.235 and θ is 19.94 degrees. The inversion results: R is 0.256, $R\cos\theta$ is 0.241 and θ is 19.89 degrees. The percentage errors are 2.3, 2.6 and 0.3 percent respectively.

Another example in Figure 9 and Figure 8 shows a synthetic dataset and its inversion results. The model is a spherical object located in a constant velocity medium. The synthetic data is generated in 3D with an offset of approximately five times the diameter of the object. The imaging is done with GOCAD. In the inversion image, an isosurface is created for the peak amplitude so that the spherical object can be shown in 3D without the diffraction events. The reflection coefficient at the normal incident position (the top of the sphere) has an error of only 3.1 percent. The position around the top of the sphere is comparably accurate except in the neighborhood of the equator, where we have no specular returns. There, the sphere is filled in by diffraction returns rather than by true specular points on the reflector. The
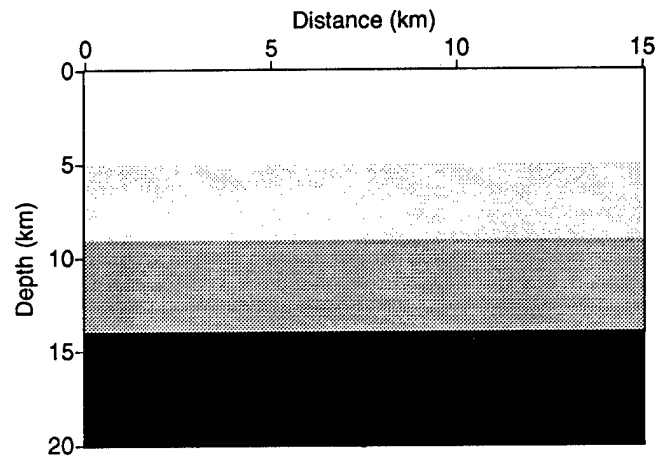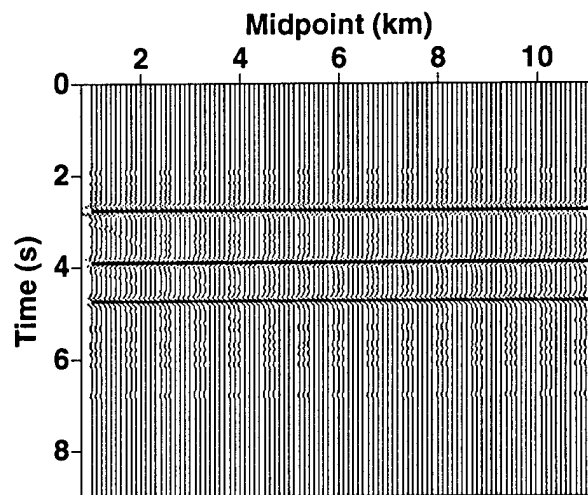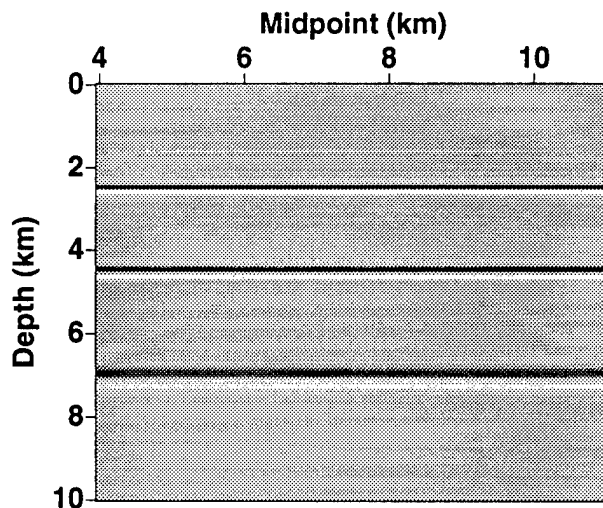
FIG. 4. Velocity Model for Example 1.

FIG. 5. Synthetic data.

FIG. 6. Reflection coefficient R.

lower half of the sphere is inaccurately positioned because the change in propagation speed across the upper sphere surface does not satisfy the criterion of being a depth dependent background velocity model. Thus, I used a constant velocity (1.5 km/s) down to the water/seabed interface and another constant below (2.0 km/s). Both are lower than the true velocity of 6 km/s in the sphere. Since the data were generated with the correct velocity, the specular returns from the lower part of the sphere came sooner than they would have at 2.0 km/s. Thus, in the imaging, the lower part of the sphere is *pulled up*, making a more elliptical surface."

CONCLUSIONS

I have described a method to calculate the amplitude weights for the 3-D common offset $v(z)$ inversion by ray tracing. The traveltime and amplitude tables generated by this method are used in (1) to perform Kirchhoff inversion. Tests on synthetic data are in progress to improve the program and the algorithm.
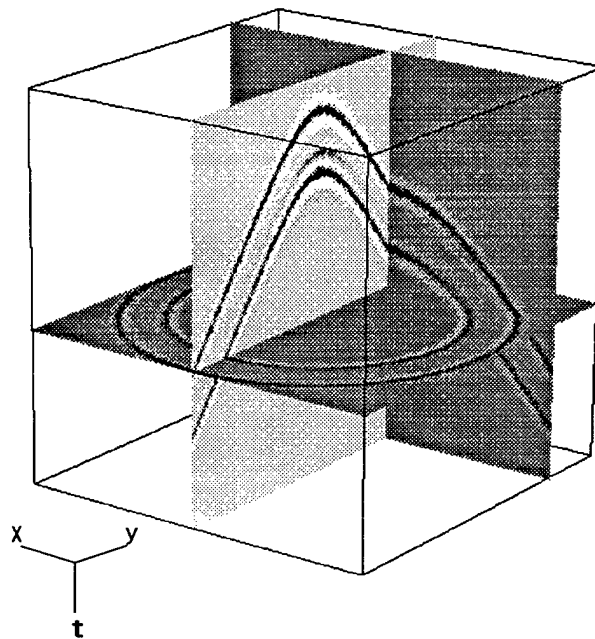
ACKNOWLEDGEMENTS

FIG. 7. Synthetic data.

REFERENCES

Bleistein, 1984, Mathematical Methods for Wave Phenomena, Acdemic Press, INC.

Bleistein, N., Cohen, J., and Hagin, F., 1987, Two and one-half dimensional Born inversion with an arbitrary reference: Geophysics, 52, 26-36.

Bleistein, N. 1986, Kirchhoff inversion for reflector imaging and sound speed and density variation. Proceedings of EAEG/SEG workshop on Deconvolution and Inversion.

Sullivan, M. and Cohen, J. K. 1987. Pre-stack Kirchhoff inversion of common offset data. Geophysics, 52, 745-754.

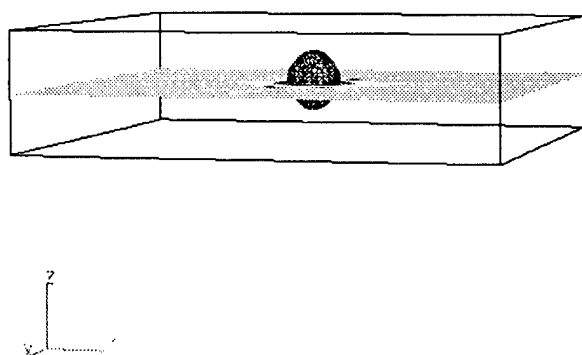FIG. 8. Inversion from the synthetic data.

REPORT DOCUMENTATION PAGE

Public reporting burden for this collection of information is estimated to average 1 hour per response, including the time for reviewing instructions, searching existing data sources, gathering and maintaining the data needed, and completing and reviewing the collection of information. Send comments regarding this burden estimate or any other aspect of this collection of information, including suggestions for reducing this burden to Washington Headquarters Services, Directorate for Information Operations and Reports, 1215 Jefferson Davis Highway, Suite 1204, Arlington, VA 22202-4302, and to the Office of Management and Budget, Paperwork Reduction Project (0704-0188), Washington, DC 20503.

1. AGENCY USE ONLY (Leave blank)	2. REPORT DATE May 1996	3. REPORT TYPE AND DATES COVERED Type A: 3/1/96-2/28/97

4. TITLE AND SUBTITLE

Amplitude calculation for 3-D common offset v(z) inversion

5. FUNDING NUMBERS

N0001-95-1-0508
PR: 21aa188---01

6. AUTHOR(S)

Meng Xu

7. PERFORMING ORGANIZATION NAME(S) AND ADDRESS(ES)

Center for Wave Phenomena
Colorado School of Mines
Golden, CO 80401

8. PERFORMING ORGANIZATION REPORT NUMBER

CWP-213

9. SPONSORING/MONITORING AGENCY NAME(S) AND ADDRESS(ES)

Ocean Acoustics Division
800 N. Quincy Street
Arlington, VA 22217-5660

10. SPONSORING/MONITORING AGENCY REPORT NUMBER

11. SUPPLEMENTARY NOTES

12a. DISTRIBUTION/AVAILABILITY STATEMENT

unclassified

12b. DISTRIBUTION CODE

13. ABSTRACT (Maximum 200 words)

The general 3-D inversion formula developed by Bleistein et al., is specialized to a depth-dependent medium. An efficient ray tracer for this model is developed to calculate the necessary constituents of the ray theory. The traveltime and amplitude tables for the inversion are computed. The motivating application for this project is detection of small objects-10cm-in shallow water-10-20m.

14. SUBJECT TERMS

Born inversion, 3-dimensional, common offset depth-dependent, amplitude

15. NUMBER OF PAGES

17

16. PRICE CODE

17. SECURITY CLASSIFICATION OF REPORT	18. SECURITY CLASSIFICATION OF THIS PAGE	19. SECURITY CLASSIFICATION OF ABSTRACT	20. LIMITATION OF ABSTRACT

NSN 7540-01-280-5500